JGP Journal of General Physiology

ARTICLE

# BK channel modulation by positively charged peptides and auxiliary γ subunits mediated by the $Ca^{2+}$-bowl site

Guanxing Chen[1], Qin Li[1], Timothy I. Webb[3], Mark A. Hollywood[3], and Jiusheng Yan[1,2]

**The large-conductance, $Ca^{2+}$-, and voltage-activated $K^+$ (BK) channel consists of the pore-forming α (BKα) subunit and regulatory β and γ subunits. The γ1–3 subunits facilitate BK channel activation by shifting the voltage-dependence of channel activation toward the hyperpolarization direction by about 50–150 mV in the absence of $Ca^{2+}$. We previously found that the intracellular C-terminal positively charged regions of the γ subunits play important roles in BK channel modulation. In this study, we found that the intracellular C-terminal region of BKα is indispensable in BK channel modulation by the γ1 subunit. Notably, synthetic peptide mimics of the γ1–3 subunits' C-terminal positively charged regions caused 30–50 mV shifts in BKα channel voltage-gating toward the hyperpolarization direction. The cationic cell-penetrating HIV-1 Tat peptide exerted a similar BK channel–activating effect. The BK channel–activating effects of the synthetic peptides were reduced in the presence of $Ca^{2+}$ and markedly ablated by both charge neutralization of the $Ca^{2+}$-bowl site and high ionic strength, suggesting the involvement of electrostatic interactions. The efficacy of the γ subunits in BK channel modulation was reduced by charge neutralization of the $Ca^{2+}$-bowl site. However, BK channel modulation by the γ1 subunit was little affected by high ionic strength and the positively charged peptide remained effective in BK channel modulation in the presence of the γ1 subunit. These findings identify positively charged peptides as BK channel modulators and reveal a role for the $Ca^{2+}$-bowl site in BK channel modulation by positively charged peptides and the C-terminal positively charged regions of auxiliary γ subunits.**

## Introduction

The large-conductance, $Ca^{2+}$-, and voltage-activated potassium (BK, Maxi-K, Slo1, or $K_{Ca1.1}$) channels are ubiquitously expressed and critically involved in various cellular and physiological processes, such as the regulation of neuron firing and transmission (Shao et al., 1999), motor coordination (Sausbier et al., 2004), learning and memory (Typlt et al., 2013), circadian rhythmicity (Meredith et al., 2006), the contractile tone of smooth muscle cells (Brenner et al., 2000), and resting $K^+$ efflux in secretory epithelial cells (Yang et al., 2017; Gonzalez-Perez et al., 2021). Mutations or dysregulation of neuronal BK channels can cause epilepsy and dyskinesia (Brenner et al., 2005; Du et al., 2005; Park et al., 2022), progressive cerebellar ataxia (Du et al., 2020), and other developmental and neurological phenotypes (Bailey et al., 2019; Liang et al., 2019).

The BK channel has a particularly large single-channel conductance and it can be activated by both membrane depolarization and elevation of intracellular free $Ca^{2+}$ ($[Ca^{2+}]_i$). The functional BK channel comprises a homotetramer of the voltage- and $Ca^{2+}$-sensing pore-forming α (BKα) subunits. Each BKα subunit has a $K^+$-selective pore gate domain, a voltage sensor domain, and a large C-terminal cytosolic region (comprising about two-thirds of the entire ~130 kD protein). The C-terminal cytosolic region possesses RCK (regulator of conductance for $K^+$) domains and two $Ca^{2+}$-sensing sites, one in the RCK1 domain formed by residues, including D362 and D367 (Zhang et al., 2010), and the other in the RCK2 domain composed of a string of negatively charged aspartic acid residues ($^{894}$DDDDD$^{898}$) known as the $Ca^{2+}$ bowl (Schreiber and Salkoff, 1997; Xia et al., 2002). The $Ca^{2+}$-bowl site forms an EF hand-like $Ca^{2+}$-binding motif that is positioned close to the assembly interface between two neighboring BKα subunits (Wu et al., 2010; Tao and MacKinnon, 2019).

BK channel function is regulated by various auxiliary β and γ subunits and by the LINGO1 protein, which are known to confer tissue-specific gating and pharmacological properties (Li and Yan, 2016; Guan et al., 2017; Gonzalez-Perez and Lingle, 2019;

[1]Department of Anesthesiology and Perioperative Medicine, The University of Texas MD Anderson Cancer Center, Houston, TX, USA; [2]Neuroscience and Biochemistry and Cell Biology Graduate Programs, MD Anderson UT Health Graduate School of Biomedical Sciences, Houston, TX, USA; [3]The Smooth Muscle Research Centre, Dundalk Institute of Technology, Dundalk, Ireland.

Correspondence to Jiusheng Yan: jyan1@mdanderson.org.

Dudem et al., 2020). The four BKγ subunits—γ1 (LRRC26), γ2 (LRRC52), γ3 (LRRC55), and γ4 (LRRC38)—have distinct capabilities in shifting the BK channel's voltage dependence of activation in the hyperpolarizing direction over an exceptionally large range of ∼145 mV (γ1), 100 mV (γ2), 50 mV (γ3), and 20 mV (γ4), in terms of the half-maximal activation voltage ($V_{1/2}$) in the absence of $Ca^{2+}$ (Yan and Aldrich, 2010, 2012). While structural insights into the mechanisms of BK channel modulation by β subunits have been acquired from cryogenic electron microscopy structures of the human BK channels in complex with β4 (Tao and MacKinnon, 2019), our understanding of the mechanisms of BK channel regulation by the auxiliary γ subunits remains very limited.

All BKγ subunits contain an N-terminal signal peptide, an extracellular leucine-rich repeat (LRR) domain, a single transmembrane (TM) segment, and a short intracellular C-terminus (Yan and Aldrich, 2010, 2012; Chen et al., 2022). The LRR domains regulate the expression, cell surface trafficking, and "all-or-none" channel-modulation functions of the BKγ subunits (Chen et al, 2022). The modulatory effects of different γ subunits on BK channel voltage dependence are determined by their single TM segments and C-terminal positively charged residue clusters (Li et al., 2015; Li et al., 2016). The single TM segment accounts for about 100 mV in $V_{1/2}$-shifting capability of the γ1 and γ2 subunits, while the intracellular C-tails, particularly the juxta-membrane positively charged residue cluster regions, contribute about 40–50 mV in $V_{1/2}$-shifting capability to the γ1 and γ3 subunits (Li et al., 2015). The positively charged residue cluster regions are also indispensable for the γ subunits' overall function in BK channel modulation, presumably because of their necessity for proper assembly of the γ subunit in the membrane (Li et al., 2015; Li et al., 2016).

In the present study, we investigated the role of the BKα subunit's intracellular region, particularly the highly negatively charged $Ca^{2+}$-bowl site, in BK channel modulation by γ subunits and the peptide mimics of their C-terminal positively charged residue regions. We identify positively charged peptides as BK channel modulators and reveal a role of the $Ca^{2+}$-bowl site in BK channel modulation by synthetic positively charged peptides and the auxiliary γ subunits.

## Materials and methods

### Expression of BK channels in HEK293 cells

HEK293 cells were cultured in Dulbecco's modified Eagle's medium with 10% fetal bovine serum, 100 IU/ml penicillin, and 100 µg/ml streptomycin in a 5% $CO_2$ incubator. The cells were transfected with plasmids using PEI "MAX" reagent (Polysciences) and subjected to electrophysiological assays 16–24 h after transfection. Recombinant cDNA constructs of human BK channel α and γ1–3 subunits were used for their heterologous expression in HEK293 cells. For expression of the BKα subunit alone, a recombinant cDNA plasmid encoding human BKα (GenBank accession number AAB65837) was used. For expression of the TM domain-only BKα, a mammalian expression plasmid of Slo1C-Kv-minT (Webb et al., 2015) generated with pcDNA3.3-TOPO vector and a truncated rabbit BKα cDNA sequence was used. This construct encodes a truncated channel similar to the previously reported Slo1C-Kv-minT channel that expressed TM domain-only mouse BKα in *Xenopus laevis* oocyte (Budelli et al., 2013). Our Slo1C-Kv-minT expresses the N-terminal TM domain (residues 1–342) of rabbit BKα with a C-terminal Kv1.4 mini-Tail (GVKESLCGTDV) tag in mammalian cells. Coexpression of the γ1 subunit with the TM domain-only BKα was achieved by cotransfection of their cDNA constructs (equal amount of plasmid DNA in weight). As described previously (Yan and Aldrich, 2010, 2012; Li et al., 2015), coexpression of BKα full-length protein and γ subunits was achieved using a BKα-γ fusion cDNA construct to facilitate 1:1 coexpression and cotranslational assembly of BKα/γ protein complexes, taking advantage of endogenous peptidase-mediated cleavage at the BKγ signal peptide region during protein translation and maturation. All mutant constructs were created using the QuikChange site-directed mutagenesis kit (Stratagene).

### Electrophysiology

The patch-clamp recording was performed with HEK293 cells, mostly in an inside-out configuration on excised plasma membrane patches or occasionally in a whole-cell configuration where specified, using symmetric intracellular and extracellular solutions containing 136 mM $KMeSO_3$, 4 mM KCl, and 20 mM HEPES, pH 7.20. The extracellular solution was supplemented with 2 mM $MgCl_2$ and the intracellular solution was supplemented with either 5 mM HEDTA without $Ca^{2+}$ to create a virtually $Ca^{2+}$-free solution or with a certain amount of $CaCl_2$ to generate the desired concentration of free $Ca^{2+}$. The free $Ca^{2+}$ concentration in the intracellular solution was measured with a $Ca^{2+}$-sensitive electrode (Orion Research). Osmolarity was measured with a Vapor Pressure Osmometer (Wescor—Vapro5520) and adjusted with sucrose if needed. Recording electrodes were pulled from borosilicate filamented glass tubes (Cat# BF150-110-10 from Sutter Instrument) with a P-1000 micropipette puller (Sutter Instrument) and polished by heat with an MF-830 microforge (Narishige) to produce a resistance of 1–2 MΩ used for inside-out recording or 2–4 MΩ used for whole-cell recording. Data were acquired with PatchMaster software (HEKA Elektronik) and an Axopatch 200B (Molecular Devices) amplifier connected to an InstruTECH ITC-18 digitizer or an EPC-10 (HEKA Elektronik) amplifier. Data were sampled at 20-µs intervals and, unless otherwise stated, filtered with the amplifiers' four-pole Bessel filter at 2 kHz (Axopatch 200B) or 2.9 kHz (EPC-10). Capacitive transients and leak currents were subtracted by a P/4 protocol at a leak holding potential of −120, −150 mV (in the presence of the γ1 subunit or $Ca^{2+}$), or −200 mV (in the presence of both the γ1 subunit and $Ca^{2+}$). Steady-state activation was expressed as normalized conductance (G/Gmax) obtained by calculation from the peak amplitudes of the tail currents (deactivation at −120 or −150 mV) and fitting with a Boltzmann function. The $V_{1/2}$ and the equivalent gating charge (z) were obtained by fitting the plot of G/Gmax versus voltage (G-V) using a single Boltzmann function $G/Gmax = 1/(1 + e^{-ZF(V-VH)/RT})$ or a double Boltzmann function $G/Gmax = Pa/(1 + e^{-ZaF(V-VHa)/RT}) + (1 - Pa)/(1 + e^{-ZbF(V-VHb)/RT})$ in which V, VH, Z, F, R, T, Pa, a, and b denote voltage, $V_{1/2}$, gating

charge (z), Faraday constant, gas constant, Kelvin temperature, portion (0–1), and component (a or b), respectively. Experimental values are reported as means ± SEM.

The peptide mimics of the BKγ subunits' C-terminal positively charged residue regions were synthesized at 95% purity with C-terminal amidation (Bio Basic) according to the amino acid sequences. The HIV-1 Tat peptide was obtained as biotin-Tat (47–57; Biotin-YGRKKRRQRRR; Cat# AS-61209; AnaSpec). The peptides were dissolved in water at 10 mM and stored at −80°C before use. Unless specified, all peptides were applied on the intracellular side of the membrane patches during patch-clamp recording via either direct addition to the bath solution or perfusion with a pressurized perfusion system (Cat# VC3-8xP from ALA Scientific Instrument). Given that the effects of the peptides (20 μM) on the voltage dependence of BK channel activation reached steady state within ∼30 s, data used to plot the G-V relationships were obtained after peptide application for ≥1 min.

### Immunoprecipitation

Immunoprecipitation of the BKα channel and the BKα/γ complex was performed as described previously (Chen et al., 2022). The cells were lysed with Tris-buffered saline (TBS) composed of 50 mM Tris (pH 7.6) and 150 mM NaCl, supplemented with 2% dodecyl-β-D-maltoside (DDM). After centrifugation (17,000 *g*) to remove insoluble fractions, the cell lysate was incubated (4°C for 2 h) with immobilized rabbit polyclonal anti-FLAG antibody (3–5 μg; Cat# F7425 from Sigma-Aldrich) covalently cross-linked to protein-A agarose beads. After three repetitive washes (10 min each time) with TBS supplemented with 2% DDM, the captured proteins were eluted from the beads with FLAG peptide (100 μg/ml). A mouse monoclonal anti-FLAG M2 antibody (Cat# F3165 from Sigma-Aldrich) at 1:1,000 dilution and a mouse monoclonal anti-V5 antibody (Cat# R96125 from Invitrogen) at 1:10,000 dilution were used for immunoblotting. A protease inhibitor cocktail (Roche) was used throughout the procedure.

### Reproducibility and data processing

All experiments were repeated to ensure reproducibility. All measurements or repeats were conducted using distinct samples or cells (i.e., biological replicates). The data were processed and plotted with Igor Pro (v5), GraphPad Prism (v8), or OriginLab (v2020). Unpaired Student's *t* test (two-tailed) was used to calculate P values.

## Results

### Requirement of the BKα subunit's C-terminal cytosolic region in BK channel modulation by the auxiliary γ1 subunit

The intracellular C-terminal tails, particularly the positively charged residue cluster regions, of the γ subunits play an important role in BK channel modulation. It is necessary to determine whether the intracellular C-terminal region of the BKα subunit is also involved in channel modulation by γ subunits. We took advantage of our previously generated rabbit BKα TM domain-only construct that encodes a channel that lacks the intracellular region after the S6 TM segment and forms $Ca^{2+}$-insensitive functional BK channels (Webb et al., 2015), comparable with the original Slo1C-Kv-minT construct (Budelli et al., 2013). Similar to the previous reports (Budelli et al., 2013; Webb et al., 2015), the voltage dependence of the TM domain-only BKα channels ($V_{1/2}$ = 260 ± 2 mV) was markedly shifted to more positive potentials compared with intact BK channels ($V_{1/2}$ = 172 ± 3 mV; Fig. 1, A and B; and Table 1). Coexpression of the γ1 subunit with the TM domain-only BKα failed to shift the voltage dependence of BK channel activation ($V_{1/2}$ = 268 ± 2 mV), although a large shift was observed with regular BK channels upon coexpression with the γ1 subunit ($V_{1/2}$ = 22 ± 3 mV; Fig. 1, A and B; and Table 1). The rabbit BKα TM domain-only construct is identical to the corresponding region of the human BKα in amino acid sequence except at a single residue (T60 in humans vs. A60 in rabbits). The loss of regulation of the TM domain-only rabbit BKα channels can only be explained by the absence of the cytosolic region in this construct. To determine whether the TM domain-only BKα can still coassemble with the γ1 subunit, we performed a coimmunoprecipitation experiment between FLAG-tagged TM domain-only BKα subunits and V5-tagged γ1 subunits using an immobilized anti-FLAG antibody. Our results (Fig. 1 C) reveal that the TM domain-only BKα subunit could be pulled down together with the γ1 subunit, suggesting a role of the BKα TM domain in complex formation with the γ1 subunit. This result agrees with our previous findings that the TM domain in the γ1 subunit is a key determinant for this subunit's association with the BKα subunit (Yan and Aldrich, 2010) and channel-modulatory function (Li et al., 2015; Li et al., 2016). Taken together, our results demonstrate that the BKα subunit's intracellular C-terminal region plays an indispensable role in BK channel modulation by the γ1 subunit, although it is not essential for overall complex formation between BKα and the γ1 subunit.

### A synthetic peptide mimic of the γ1 subunit's C-terminal positively charged region activated and blocked BK channels

Given the importance of the positively charged residue regions of the γ subunits' intracellular C-tails in BK channel modulation, we synthesized peptide mimics of the corresponding regions and determined their effects on BKα channels. We first examined the effects of different concentrations of the synthetic γ1 peptide (TACRARRRLR) on BKα channels in the virtual absence of $[Ca^{2+}]_i$. Upon perfusion of the synthetic peptide on the intracellular side of the patches, we observed two effects on the BK currents, namely blockade of the outward currents at positive voltages (e.g., 140 mV) and enhancement of the inward tail currents at negative voltages (e.g., −120 mV; Fig. 2 A). The latter indicated an increase in the channel's open probability and thus a channel-activating effect of the peptide. Although both the blockade and activating effects were close to maximum in the presence of 5–20 μM peptide, they differed in their responses to peptide at lower concentrations. The onset of the blockade effect occurred only at peptide concentrations above 1 μM, whereas the tail current enhancement was evident at 0.2 μM (Fig. 2, B and C). We also consistently noted an enhancement of outward currents in the presence of 0.2 and 1 μM peptide (Fig. 2 B).

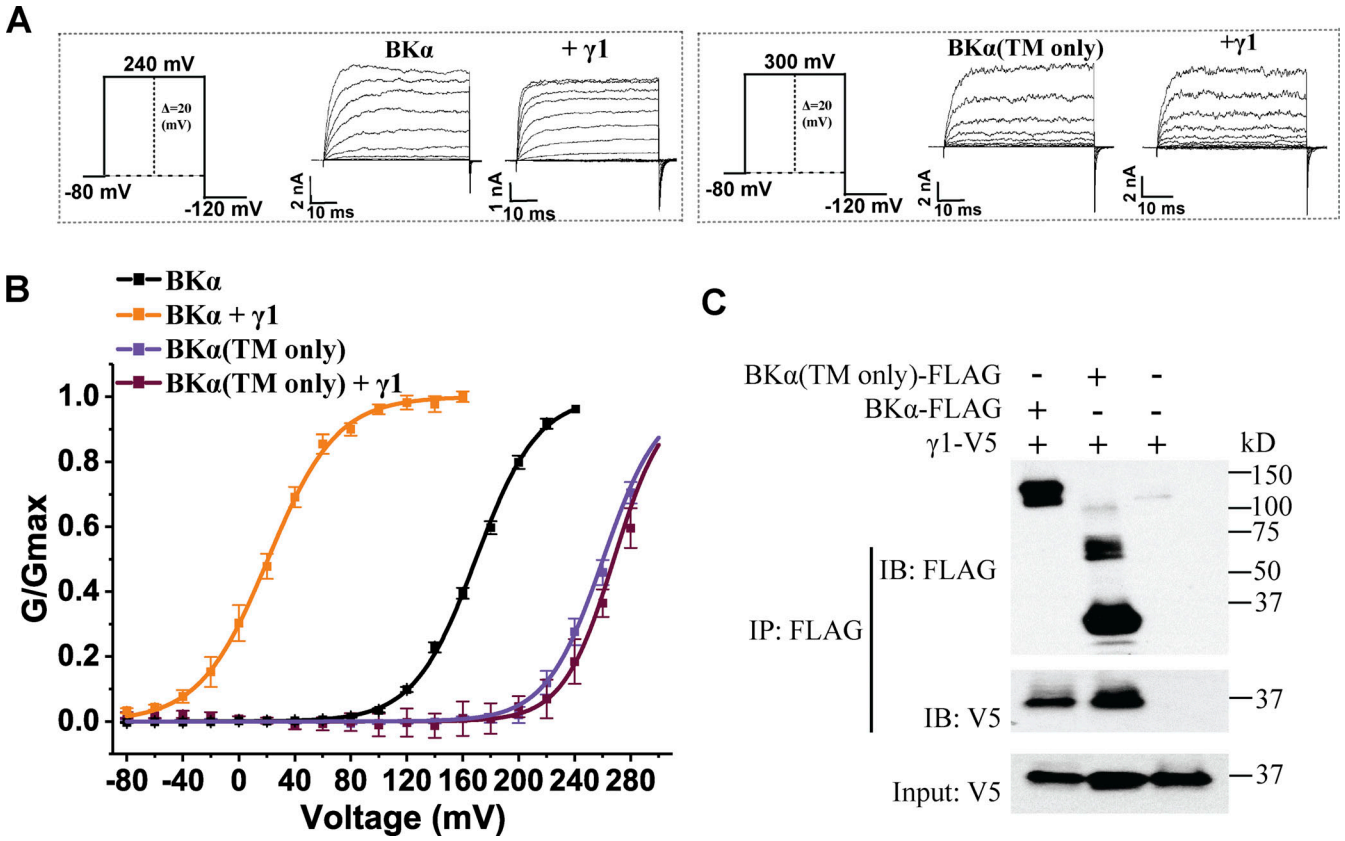


Figure 1. **Role of the C-terminal cytosolic region of the BKα subunit for BK channel modulation by the auxiliary γ1 subunit. (A)** Representative current traces of BK channels formed by WT (no label) and the TM-only BKα subunit in the absence and presence of the γ1 subunit in response to depolarization of the membrane potential from −80 mV in 20-mV steps. **(B)** Voltage dependence of BK channel activation for channels formed by WT and the TM-only BKα subunit in the absence and presence of the γ1 subunit. **(C)** Immunoprecipitation of the γ1 subunit with WT and the TM-only BKα subunit. For all plots of the G/Gmax–voltage (G-V) relationships here and in other figures, the number of repeats (*n*) used in plotting the individual G-V curve is the same as that of the corresponding data listed in Table 1. Source data are available for this figure: SourceData F1.

Furthermore, the time-dependency of the peptide's two effects was distinct. Upon perfusion of 5 μM γ1 peptide, enhancement of the inward tail currents occurred rapidly with a τ of ∼5 s, whereas blockade of the outward currents appeared to be more than twofold slower as evidenced by the τ = ∼13 s for the blockade effect (Fig. 2, D–F). The enhancement of the tail currents was accompanied by an increase in the τ of the tail current decay, indicating the slowing of channel closure (Fig. 2, A and G). The peptide-induced enhancement of the tail currents was reversed within 5 min upon perfusion of a solution without peptide whereas the blockade of outward currents mostly remained (Fig. 2, H–J). These results indicated that the peptide's blockade and activating effects on BK channels were largely independent. At higher concentrations (e.g., 50 μM), the peptide appeared to produce some additional blockade effect on inward currents as a decrease in inward currents was observed (Fig. 2 C). Therefore, we chose a peptide concentration of 20 μM for the rest of the study to maximize the channel activating effect, minimize the blockade effect on tail currents, and avoid solubility issues with the peptide. It was not surprising to observe channel blockade with these peptides since positively charged small chemicals and peptides (e.g., tetrabutylammonium and enhanced ball peptide) were previously reported to reach and block BK channel pore from the intracellular side in a voltage-dependent manner (Li and Aldrich, 2006). However, since full-length γ subunits have not been shown to block BK channels, we focused on investigating the activation effects of these positively charged synthetic peptides derived from C-tails of the γ subunits.

### Synthetic peptide mimics of the γ subunits' C-terminal positively charged regions and HIV-1 Tat induced shifts in the BKα channel's voltage gating in the hyperpolarization direction

When we plotted the voltage dependence of channel activation (Fig. 3, A and B; and Table 1), we observed that the γ1 peptide (20 μM) induced a −48 mV shift in $V_{1/2}$ (172 ± 3 vs. 124 ± 3 mV in the absence and presence of the peptide, respectively). Similarly, intracellular application of the synthetic γ3 peptide mimic (NCCHRWSK) at 20 μM resulted in a −35 mV shift in the $V_{1/2}$ ($V_{1/2}$ = 137 ± 1 mV in the presence of the peptide; Fig. 3 B and Table 1). Likewise, the synthetic γ2 peptide mimic (VLYQNTRHK) at 20 μM induced a significant −37 mV shift in $V_{1/2}$ ($V_{1/2}$ = 135 ± 1 mV in the presence of the peptide; Fig. 3 B and Table 1). The shifting capacity of the γ1 peptide is likely related to the abundance of positive charges since the removal of four

Table 1 **Boltzmann-fit parameters of the voltage-dependent BK channel activation in the absence and presence of the γ subunit and/or synthetic peptides**

| Expression | Boltzmann fit parameters | | |
|---|---|---|---|
| | $V_{1/2}$ (mV) | z | n[a] |
| $BK\alpha^{(TM\text{-}only)}$ | 260 ± 2 | 1.43 ± 0.1 | 4 |
| $BK\alpha^{(TM\text{-}only)}$ + γ1 | 269 ± 2 | 1.5 ± 0.16 | 4 |
| BKα | 172 ± 3 | 1.75 ± 0.09 | 9 |
| BKα-γ1 | 22 ± 3 | 1.75 ± 0.09 | 7 |
| BKα-γ2 | 61 ± 3 | 1.17 ± 0.07 | 8 |
| BKα-γ3 | 115 ± 2 | 1.36 ± 0.05 | 6 |
| BKα (10 μM $Ca^{2+}$) | 17 ± 2 | 1.14 ± 0.06 | 10 |
| BKα-γ1 (10 μM $Ca^{2+}$) | −71 ± 1 | 0.85 ± 0.02 | 4 |
| BKα-γ2 (10 μM $Ca^{2+}$) | −62 ± 2 | 1.28 ± 0.12 | 7 |
| BKα-γ3 (10 μM $Ca^{2+}$) | −17 ± 2 | 1.69 ± 0.15 | 5 |
| $BK\alpha^{(D362A/D367A/5D5N)}$ | 163 ± 4 | 1.12 ± 0.11 | 3 |
| $BK\alpha^{(D362A/D367A/5D5N)}$-γ1 | 56 ± 5 (76%)[b]<br>160 ± 13 (24%)[b] | 1.29 ± 0.05<br>1.17 ± 0.12 | 5 |
| $BK\alpha^{(D362A/D367A/5D5N)}$-γ2 | 127 ± 13 | 0.73 ± 0.02 | 4 |
| $BK\alpha^{(D362A/D367A/5D5N)}$-γ3 | 174 ± 9 | 0.93 ± 0.16 | 6 |
| $BK\alpha^{(D362A/D367A)}$ | 175 ± 2 | 1.07 ± 0.02 | 5 |
| $BK\alpha^{(D362A/D367A)}$-γ1 | 43 ± 4 | 1.37 ± 0.16 | 6 |
| $BK\alpha^{(D362A/D367A)}$-γ2 | 65 ± 3 | 1.08 ± 0.12 | 10 |
| $BK\alpha^{(D362A/D367A)}$-γ3 | 133 ± 2 | 1.58 ± 0.19 | 5 |
| $BK\alpha^{(5D5N)}$ | 183 ± 2 | 1.32 ± 0.04 | 7 |
| $BK\alpha^{(5D5N)}$-γ1 | 85 ± 4 | 1.67 ± 0.73 | 5 |
| $BK\alpha^{(5D5N)}$-γ2 | 131 ± 2 | 0.91 ± 0.06 | 5 |
| $BK\alpha^{(5D5N)}$-γ3 | 182 ± 1 | 1.38 ± 0.11 | 5 |
| BKα + 20 μM γ1 peptide | 124 ± 3 | 1.39 ± 0.04 | 12 |
| BKα + 20 μM γ2 peptide | 135 ± 1 | 1.34 ± 0.17 | 7 |
| BKα + 20 μM γ3 peptide | 137 ± 1 | 1.14 ± 0.05 | 4 |
| BKα + 20 μM γ1-Δ4R peptide | 145 ± 1 | 1.19 ± 0.03 | 13 |
| BKα + 20 μM HIV-1 Tat peptide | 127 ± 2 | 1.49 ± 0.05 | 5 |
| BKα (whole-cell recording) | 188 ± 3 | 0.82 ± 0.02 | 5 |
| BKα + 20 μM HIV-1 Tat peptide (whole-cell recording) | 183± 7 | 0.85 ± 0.03 | 5 |
| BKα + 200 μM HIV-1 Tat peptide (whole-cell recording) | 162 ± 3 | 0.71 ± 0.03 | 5 |
| BKα + 20 μM HIV-1 Tat peptide (in pipette) | 179 ± 6 | 1.37 ± 0.06 | 5 |
| BKα (20 μM $Ca^{2+}$) | 2 ± 4 | 1.53± 0.34 | 3 |
| BKα + 20 μM γ1 peptide (20 μM $Ca^{2+}$) | −25 ± 4 | 1.66 ± 0.12 | 8 |
| BKα (1 mM $Ca^{2+}$) | −60 ± 6 | 2.1 ± 0.12 | 3 |
| BKα + 20 μM γ1 peptide (1 mM $Ca^{2+}$) | −72 ± 3 | 2.2 ± 0.2 | 3 |

Table 1 **Boltzmann-fit parameters of the voltage-dependent BK channel activation in the absence and presence of the γ subunit and/or synthetic peptides (*Continued*)**

| Expression | Boltzmann fit parameters | | |
|---|---|---|---|
| | $V_{1/2}$ (mV) | z | n[a] |
| $BK\alpha^{(5D5N)}$ + 20 μM γ1 peptide | 169 ± 3 | 1.32 ± 0.06 | 7 |
| $BK\alpha^{(5D5N)}$ + 20 μM γ2 peptide | 165 ± 5 | 1.12 ± 0.09 | 4 |
| $BK\alpha^{(5D5N)}$ + 20 μM γ3 peptide | 180 ± 3 | 1.25 ± 0.19 | 6 |
| BKα (1 M $KMeSO_3$, 1,630 mOsm/kg) | 112 ± 3 | 1.13 ± 0.065 | 5 |
| BKα + 20 μM γ1 peptide (1 M $KMeSO_3$, 1,630 mOsm/kg) | 122 ± 6 | 1.105 ± 0.18 | 5 |
| BKα (50 mM $KMeSO_3$, 302 mOsm/kg) | 182 ± 3 | 1.13 ± 0.07 | 5 |
| BKα + 20 μM γ1 peptide (50 mM $KMeSO_3$, 302 mOsm/kg) | 132 ± 4 | 1.16 ± 0.05 | 5 |
| BKα (140 mM $KMeSO_3$, 1,650 mOsm/kg) | 172 ± 2 | 1.51 ± 0.28 | 4 |
| BKα + 20 μM γ1 peptide (140 mM $KMeSO_3$, 1,650 mOsm/kg) | 132 ± 3 | 1.43 ± 0.06 | 4 |
| BKα-γ1 (1 M $KMeSO_3$, 1,630 mOsm/kg) | −31 ± 5 | 0.95 ± 0.21 | 5 |
| BKα-γ1 + 20 μM γ1 peptide | −18 ± 5 | 1.32 ± 0.05 | 5 |

Unless indicated, recordings were done in the virtual absence of intracellular free $Ca^{2+}$ and an inside-out configuration.
[a]The number of recorded excised inside-out patches from different HEK293 cells.
[b]Portion of the $V_{1/2}$ component obtained by fitting with a double Boltzmann function.

arginines in the middle of the γ1 peptide decreased the peptide-induced shift in $V_{1/2}$ by 21 mV ($V_{1/2}$ = 145 ± 0.8 mV in the presence of the TACRALR peptide; Fig. 3 C and Table 1). With only two positively charged arginines or lysines in the synthetic γ1-Δ4R, γ2, and γ3 peptides, the blockade of outward currents was alleviated in comparison with the blockade caused by the synthetic γ1 peptide mimic, which contained six arginines.

We next determined if the BK channel–activating effect also occurred with other positively charged peptides, so we examined the effects of the well-known, cationic cell-penetrating HIV-1 Tat peptide (GRKKRRQRRRPQ; Rizzuti et al., 2015) on currents. We found (Fig. 3 D and Table 1) that 20 μM of this peptide induced a −45 mV shift in $V_{1/2}$ to 127 ± 2 mV, just like the effects of the γ1 peptide. These results demonstrated that peptides with two or more positive charges, in general, can act as an activator of BK channels. Given the membrane-penetrating property of the positively charged peptides, we applied the HIV-1 Tat peptide from the extracellular side in both inside-out and whole-cell recordings to determine whether the peptide exerts its channel-activating effect from the extracellular side or via intramembrane interactions. We observed little effect of the

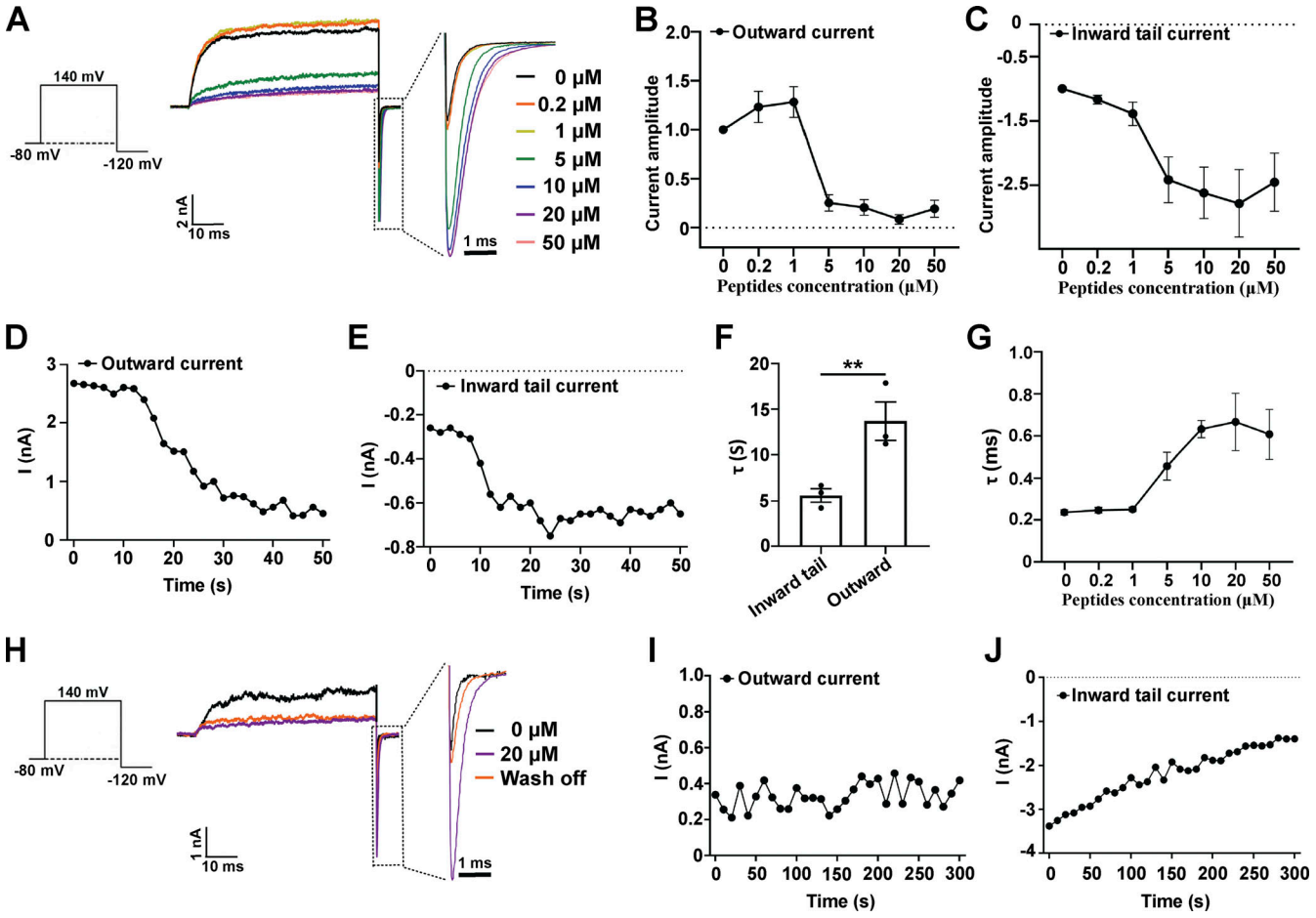


Figure 2. **Effects of a synthetic peptide mimic of the γ1 subunit's C-terminal positively charged region on BKα channels. (A)** The effect of different concentrations of γ1 peptide on BKα channel currents elicited by activation at 140 mV and then deactivation at −120 mV. The current data were low-pass filtered at 10 kHz. **(B)** Normalized outward current amplitudes of BKα channels in the presence of different concentrations of the γ1 peptide. **(C)** Normalized inward tail current amplitudes of BKα channels in the presence of different concentrations of the γ1 peptide. **(D and E)** Representative time-dependence of the maximal amplitude of the BKα channel outward currents (140 mV; D) and inward tail currents (−120 mV; E) upon application of 5 μM γ1 peptide. **(F)** Averaged rates (τ) of the peptide-induced changes in BKα channel inward tail currents and outward currents as shown in D and E. Unpaired Student's *t* test (two-tailed) was used to calculate P values. ** is for P values ≤ 0.01 (P = 0.0073). *n* = 3. **(G)** The effect of different concentrations of the γ1 peptide on the averaged kinetics (τ) of BKα channel deactivation (inward tail currents) at −120 mV. **(H)** The effect of peptide wash-off on the BKα channel currents was elicited by activation at 140 mV and then deactivation at −120 mV. The γ1 peptide was applied at 20 μM for 1 min and then washed for 5 min. The current data were low-pass filtered at 10 kHz. **(I and J)** Representative time-dependence of the maximal amplitude of the BKα channel outward currents (140 mV; I) and inward tail currents (−120 mV; J) upon solution perfusion without peptide. The excised patches were pretreated (perfusion) with 20 μM γ1 peptide for 1 min. All BK channel currents were recorded in the virtual absence of $[Ca^{2+}]_i$. Error bars represent ± SEM.

Tat peptide (20 μM) on BK channels when it was included in the pipette solution in inside-out recordings (Fig. 3 F and Table 1) or perfused on the extracellular side in whole-cell recordings (Fig. 3 G and Table 1). Thus, the Tat peptide mainly exerts its channel-activating function via the intracellular side. Given that high concentrations of HIV-1 Tat have been used as a vehicle in cellular delivery (Niesner et al., 2002; Aoki and Tosato, 2004), we treated the cells with 200 μM HIV-1 Tat peptide overnight and performed whole-cell recording. Under this condition, we observed a −26 mV shift in $V_{1/2}$ ($V_{1/2}$ was 162 ± 3 mV, compared to the untreated cells where it was 188 ± 4 mV; Fig. 3 G and Table 1), suggesting that cationic cell–penetrating peptides could accumulate inside cells and modulate BK channels when used at high concentrations.

### BK channel activation by positively charged peptides likely occurs via electrostatic interactions with the $Ca^{2+}$-bowl site

In the large intracellular domain of BKα subunits, the characteristic, negatively charged, $Ca^{2+}$-bowl site is defined by a string of eight negatively charged residues ($^{892}$DQDDDDDPDTE$^{902}$). To determine whether the modulation of BK channels by synthetic peptides was mediated by the $Ca^{2+}$-bowl site via electrostatic interactions, we first tested the effects of $Ca^{2+}$ on BK channel modulation by the peptides. As the $Ca^{2+}$ concentration increased, the BK channel $V_{1/2}$-shifting capability of the γ1 peptide was reduced. The BK channel $V_{1/2}$-shifting capability of the γ1 peptide was reduced to 27 and 12 mV in the presence of 20 μM and 1 mM $Ca^{2+}$, respectively (Fig. 4, A and B; and Table 1). We next examined the effects of charge neutralization through mutation of five consecutive Asp residues, D894N/D895N/D896N/D897N/

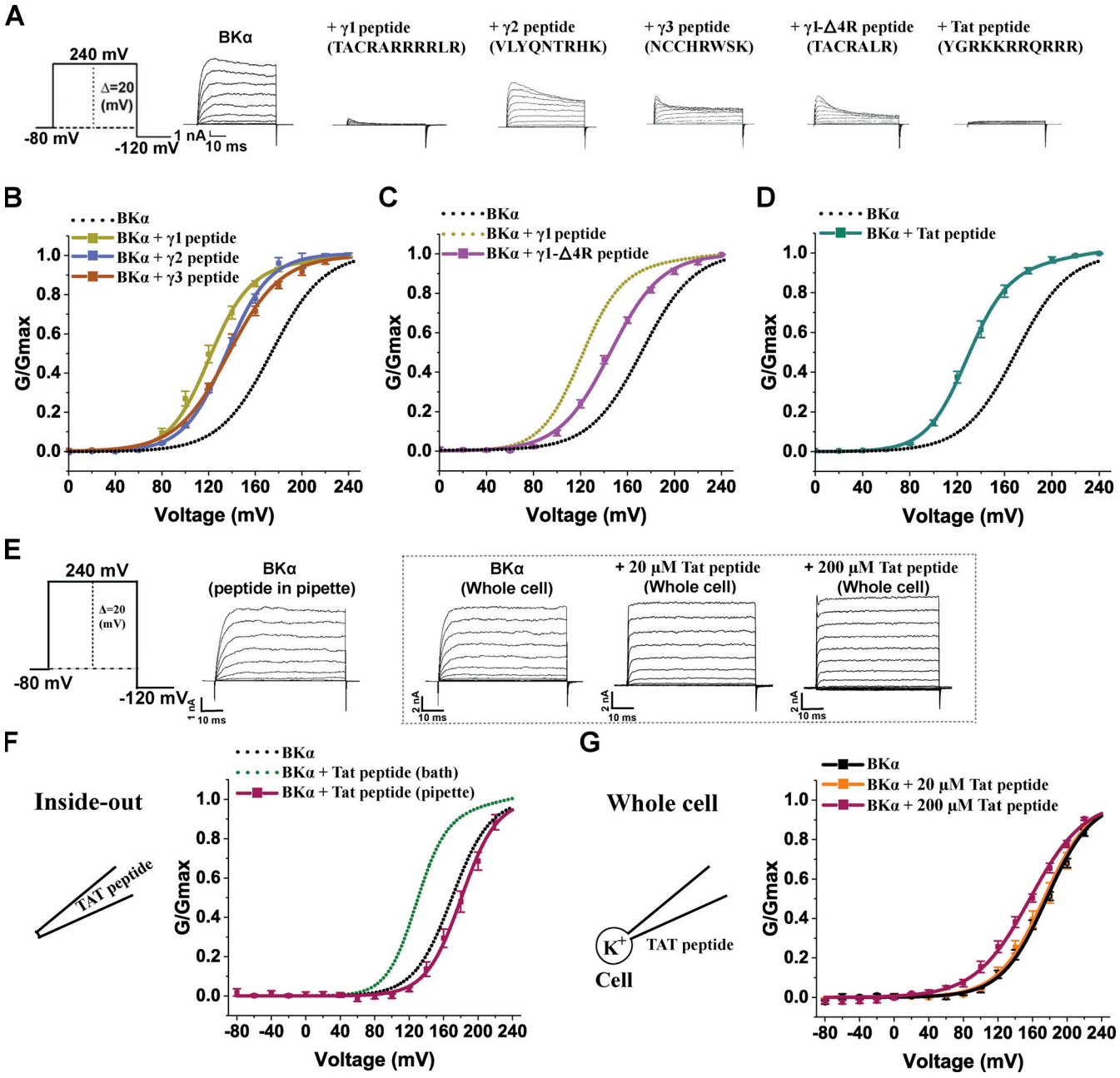


Figure 3. **Effects of synthetic peptide mimics of the γ subunits' C-terminal positively charged regions and of HIV-1 Tat on BKα channels.** **(A)** Representative traces of recorded BKα channel currents in response to depolarization of the membrane potential from −80 to 240 mV in 20 mV steps in the presence of different synthetic peptides. For comparison of the blockade in outward currents, the maximal amplitudes of tail currents were normalized to that without peptides. **(B–D)** Voltage dependence of BK channel activation in the presence of 20 μM γ1–γ3 (B), γ1-Δ4R (C), and HIV-1 Tat (D) peptides. The peptides were applied with a perfusion system. **(E)** Representative current traces of BKα channels in the presence of extracellularly applied HIV-1 Tat peptide in response to depolarization of the membrane potential from −80 to 240 mV in 20 mV steps. **(F)** Voltage dependence of BKα channel activation with 20 μM HIV-1 Tat peptide included in the inside-out recording pipette solution. **(G)** Voltage dependence of BKα channel activation with 20 or 200 μM HIV-1 Tat peptide applied on the extracellular side in whole-cell recording configuration. For the 200 μM HIV-1 Tat peptide condition, the peptide was added to the cell culture medium overnight and also included in bath solution during recording. All BK channel currents were recorded in the virtual absence of $[Ca^{2+}]_i$. Error bars represent ± SEM.

D898N (5D5N), in the $Ca^{2+}$-bowl site on BK channel modulation by the γ peptides. With the 5D5N mutation, the peptides remained effective at blocking BK channel outward currents at positive potentials (Fig. 4 A) whereas the channel-activating effects of the synthetic γ1, γ2, and γ3 peptides were decreased by 71, 51, and 74%, respectively (Fig. 4, B and D–F; and Table 1). A comparison of the tail currents before and after the application of the peptide revealed that the effects of the γ1 peptide on tail current amplitude and kinetics of the 5D5N mutant channel were greatly reduced as compared with the WT channels (Fig. 4

B). For both WT and 5D5N mutant channels, when the channels were maximally activated at high voltages (e.g., 240 mV), the peak amplitudes of the tail currents in the presence and absence of the peptides were largely similar (Fig. 4 B), suggesting that the blockade effect of 20 μM peptide on tail currents at a very negative voltage (−120 mV) was limited. These results demonstrate an essential role for the $Ca^{2+}$-bowl site in BK channel activation by synthetic peptides that mimic the positively charged regions of γ subunits. The results also strongly support the involvement of distinct mechanisms underlying the peptide's blockade and activating effects on BK channels. To evaluate whether electrostatic interactions at the $Ca^{2+}$ bowl site were involved in the stimulatory effects of the peptides, we examined the effects of high ionic strength on the response. We found that increasing ionic strength to 1 M $KMeSO_3$ fully abolished the channel-activating effect of the γ1 peptide (Fig. 5, A and B; and Table 1), whereas neither a reduction in ionic strength from regular 140 mM $KMeSO_3$ to 50 mM $KMeSO_3$ nor a change in osmolality had any significant effect (Fig. 5, A and C; and Table 1). These results indicate that positively charged peptides activate BK channels likely via electrostatic interactions with the negatively charged $Ca^{2+}$-bowl site. The residual responses of the 5D5N mutant channels to the γ peptides could be due to the remaining negatively charged residues (D892, D900, and E902) in the $Ca^{2+}$-bowl region or due to other negatively charged region(s), e.g., the $Ca^{2+}$-binding site on the RCK1 domain.

### Charge neutralization of the $Ca^{2+}$-bowl site reduced channel modulation by γ subunits

To determine whether the γ subunits' C-terminal positively charged regions function similarly to their peptide mimics in BK channel modulation, we investigated the effects of charge neutralization mutations of the $Ca^{2+}$-binding sites and $Ca^{2+}$ on BK channel modulation by intact γ subunits. We assessed the modulatory effects of the γ1–3 subunits on the $Ca^{2+}$-insensitive BK channel mutant whose $Ca^{2+}$ binding in both RCK1 and RCK2 domains was nullified by the combinational D362A/D367A/5D5N mutations. We observed that this "triple mutant" (D362A/D367A/5D5N) reduced the maximal BK channel $V_{1/2}$ shifting capabilities of the γ1 and γ2 subunits by about 43 (fitted with double Boltzmann) and 75 mV, respectively, and a complete loss of the γ3 subunit-induced shift of $V_{1/2}$ (Fig. 6, A–E; and Table 1). The D362A/D367A/5D5N mutation induced a significant portion (24%) of the channels to behave as BKα-only channels, and the resulting G-V curves were best fit with a double Boltzmann function to account for the "all-or-none" nature of γ modulated channels (Gonzalez-Perez et al., 2014). We examined the modulatory effects of the γ1–3 subunits on the BKα $Ca^{2+}$ binding–defective mutants D362A/D367A (RCK1) and 5D5N (RCK2), separately. We observed that the 5D5N mutation appeared to have a predominant effect on BK channel modulation by the γ1–3 subunits (Fig. 6, A–E) compared with the RCK1 mutant. The D362A/D367A mutation caused no change and a reduction of 18 and 15 mV in the shifts of BK channel $V_{1/2}$ induced by the γ2, γ1, and γ3 subunits, respectively, (Fig. 6, A–E; and Table 1). However, in BK channels with the 5D5N mutation, the shift in $V_{1/2}$ induced by the γ1, γ2, and γ3 subunits, was markedly reduced by 58, 65, and 62 mV, respectively (Fig. 6, A–E; and Table 1). Similar to that observed with the TM domain-only BKα mutant, we observed no significant reduction in the association of the γ1 subunit with the 5D5N mutant as compared with the WT BKα subunit. The γ1 subunit was still pulled down with the 5D5N mutant during coimmunoprecipitation using an anti-BKα antibody (Fig. 6 F).

### $Ca^{2+}$ reduced the γ subunit-induced shifts in the voltage dependence of BK channel activation

We previously reported that the shifts in BK channel $V_{1/2}$ caused by the γ2 and γ3 subunits were reduced by ∼30–50 mV in the presence of a concentration (26 μM) of $[Ca^{2+}]_i$ compared with those obtained in the absence of $Ca^{2+}$ (Yan and Aldrich, 2012). In the presence of 10 μM $Ca^{2+}$, we report here that the shifts in BK channel $V_{1/2}$ caused by γ1, γ2, and γ3 decreased by 62, 32, and 23 mV, respectively, compared with those obtained in the absence of $Ca^{2+}$ (Fig. 7, A–E; and Table 1). To help understand the potential mechanisms of the $Ca^{2+}$ effect on BK channel modulation by γ subunits, we performed mathematic modeling analysis of the impact of $Ca^{2+}$ on BK channel modulation by the γ1 subunit based on the Horrigan–Aldrich (HA) allosteric model of BK channel gating by voltage and $Ca^{2+}$ (Horrigan and Aldrich, 2002). For our analysis, we assumed that the major effect of the γ1 subunit is an ∼20-fold increase in the allosteric coupling (D factor) between the voltage sensor and the pore gate (Yan and Aldrich, 2010). According to the HA model (Horrigan and Aldrich, 2002), the relationship between the channel's open probability ($P_o$) and voltage/$Ca^{2+}$ can be described by three allosteric coupling factors (C, D, E) and three equilibrium constants (J, K, L) with the equations: $P_o = \frac{L(1+KC+JD+JKCDE)^4}{L(1+KC+JD+JKCDE)^4+(1+J+K+JKE)^4}$; $L = L_0 exp\left(\frac{Z_L V}{KT}\right)$; $J = J_0 exp\left(\frac{Z_J V}{KT}\right)$; and $K = \frac{[Ca^{2+}]}{K_D}$. $L_0$ and $J_0$ are zero voltage values of L and J, respectively. $Z_L$ and $Z_J$ are partial charges associated with channel opening and voltage sensor activation, respectively. $K_D$ is the $Ca^{2+}$ dissociation constant when the channel is closed and voltage sensors are not activated. The HA model predicts that the shift in $V_{1/2}$ induced by an increase in D factor from 21 to 412 is significantly less at 10 μM $Ca^{2+}$ ($|\Delta V_{1/2}|$ = 120 mV) as compared to that in the absence of $Ca^{2+}$ ($|\Delta V_{1/2}|$ = 158 mV; Fig. 7 F), which could partially explain the observed effect of $Ca^{2+}$ on the voltage dependence of BK channel activation in the presence of the γ1 subunit.

### High ionic strength and positively charged peptides had little effect on BK channel modulation by the γ1 subunit

Given that the γ subunits and synthetic γ peptides both modulate BK channels in a manner sensitive to charge neutralization of the $Ca^{2+}$-bowl site, we next investigated whether the γ subunits and positively charged peptides interact with the $Ca^{2+}$-bowl site in a similar manner. If the two interactions are similar, we would expect to observe that (1) BK channel modulation by the γ subunit would be reduced under high ionic strength and (2) the peptides may be less effective in modulating the BKα/γ channel complex than modulating the BKα only channel if the γ subunit and peptides compete in their interactions with the $Ca^{2+}$-bowl sites. However, we observed that BK channel

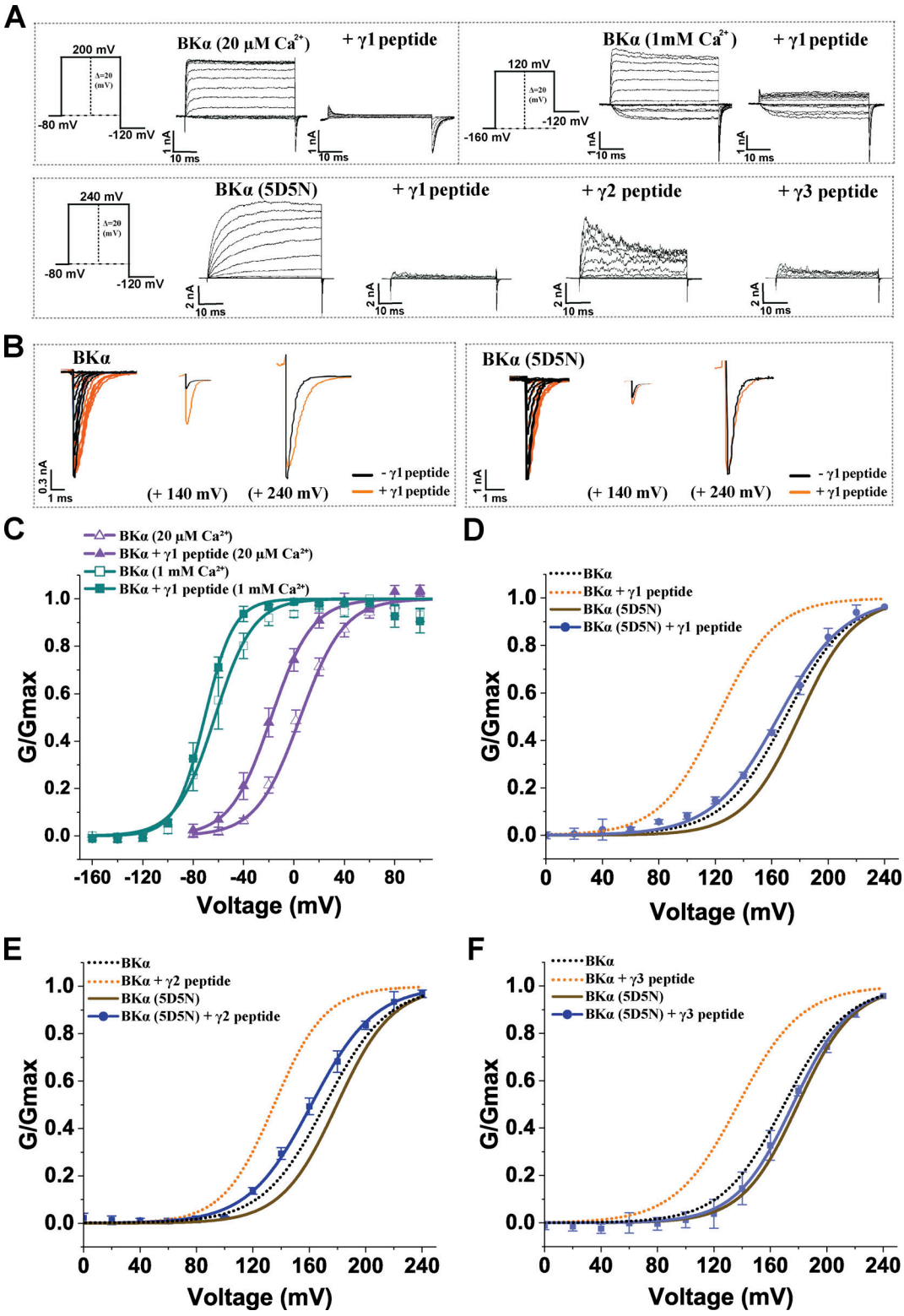


Figure 4. **The effects of $Ca^{2+}$ and charge neutralization of the $Ca^{2+}$-bowl site on BKα channel modulation by the synthetic γ peptide mimics.** **(A)** Representative current traces of BKα WT (no label) and 5D5N mutant channels in response to depolarization of the membrane potential from −80 or −160 mV in 20-mV steps for selected expression constructs. **(B)** The overlayed inward tail currents of BKα WT and 5D5N mutant channels before and after application of 20 μM γ1 peptide. Currents elicited by activation at all voltages, 140 mV, and 240 mV are shown from left to right. The current data were low-pass filtered at 10 kHz. **(C)** Voltage dependence of BKα channel activation in the presence of 20 μM γ1 peptide at 20 μM and 1 mM $Ca^{2+}$. **(D–F)** Voltage dependence of BKα 5D5N mutant channel activation in the presence of the 20 μM γ1 (D), γ2 (E), or γ3 (F) peptide at virtual 0 $Ca^{2+}$. Error bars represent ± SEM.

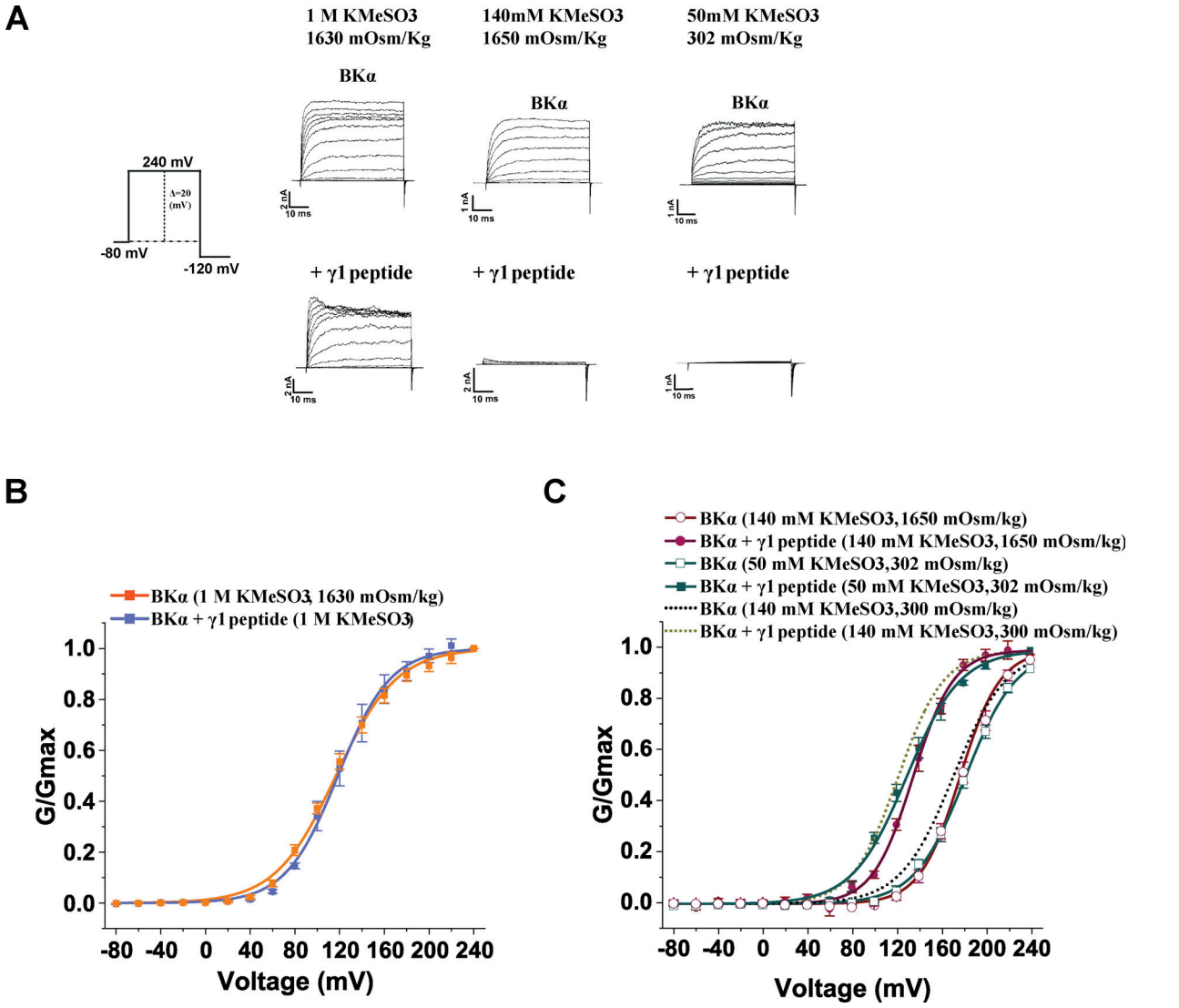


Figure 5. **The effects of ionic strength on BKα channel modulation by the synthetic γ1 peptide mimic. (A)** Representative current traces of BK channels formed by the BKα subunit under different intracellular conditions (peptide treatment and ionic strength) in response to depolarization of the membrane potential. **(B)** Voltage dependence of BKα channel activation with intracellular solutions of 1 M $KMeSO_3$ in the absence and presence of 20 µM γ1 peptide. **(C)** Voltage dependence of BKα channel activation with intracellular solutions of different ionic strength or osmolarity in the absence and presence of 20 µM γ1 peptide. The peptide was applied with a perfusion system. Currents were recorded in the virtual absence of $[Ca^{2+}]_i$. Osmolarity was adjusted by sucrose for the low ionic strength solution of 50 mM $KMeSO_3$ and the high osmolarity solution containing 140 mM $KMeSO_3$. Error bars represent ± SEM.

modulation by the γ1 subunit was not significantly affected in 1 M $KMeSO_3$, as the shift in $V_{1/2}$ ($\Delta V_{1/2}$ = 143 mV) was comparable to that recorded in 140 mM $KMeSO_3$ ($\Delta V_{1/2}$ = 150 mV; Fig. 8, A and B; and Table 1). Moreover, 20 µM γ1 peptide effectively modulated the BKα/γ1 channel, producing about −40 mV shift in $V_{1/2}$ (Fig. 8, A and C; and Table 1). Therefore, we conclude that the intact γ1 subunit, particularly its C-terminal positively charged region, and the corresponding synthetic peptide mimic differ in the mechanisms underlying their modulation of BK channels albeit both involve the $Ca^{2+}$ bowl of the BK channel.

## Discussion

Previously, we identified the single TM segment and the adjacent intracellular positively charged residue cluster as the two key determinants for the different modulatory effects of the four γ subunits on the BK channel's voltage dependence of channel activation (Li et al., 2015; Li et al., 2016). We found that the positively charged clusters play a dual role as they are not only indispensable for the overall function of the γ subunits but also contribute an additional ∼40 mV in BK channel $V_{1/2}$-shifting capability to the γ1 and γ3 subunits. In the present study, we found that the intracellular C-terminal region of BKα is also indispensable for BK channel modulation by the γ subunit. Notably, charge neutralization of the BKα's $Ca^{2+}$-bowl site was accompanied by a marked reduction in the BK channel $V_{1/2}$-shifting capability of the γ1–3 subunits. The synthetic peptides that mimic the γ subunits' positively charged residue clusters also induced an ∼30–50 mV shift in BK channel $V_{1/2}$ when applied on the intracellular side of the membrane.

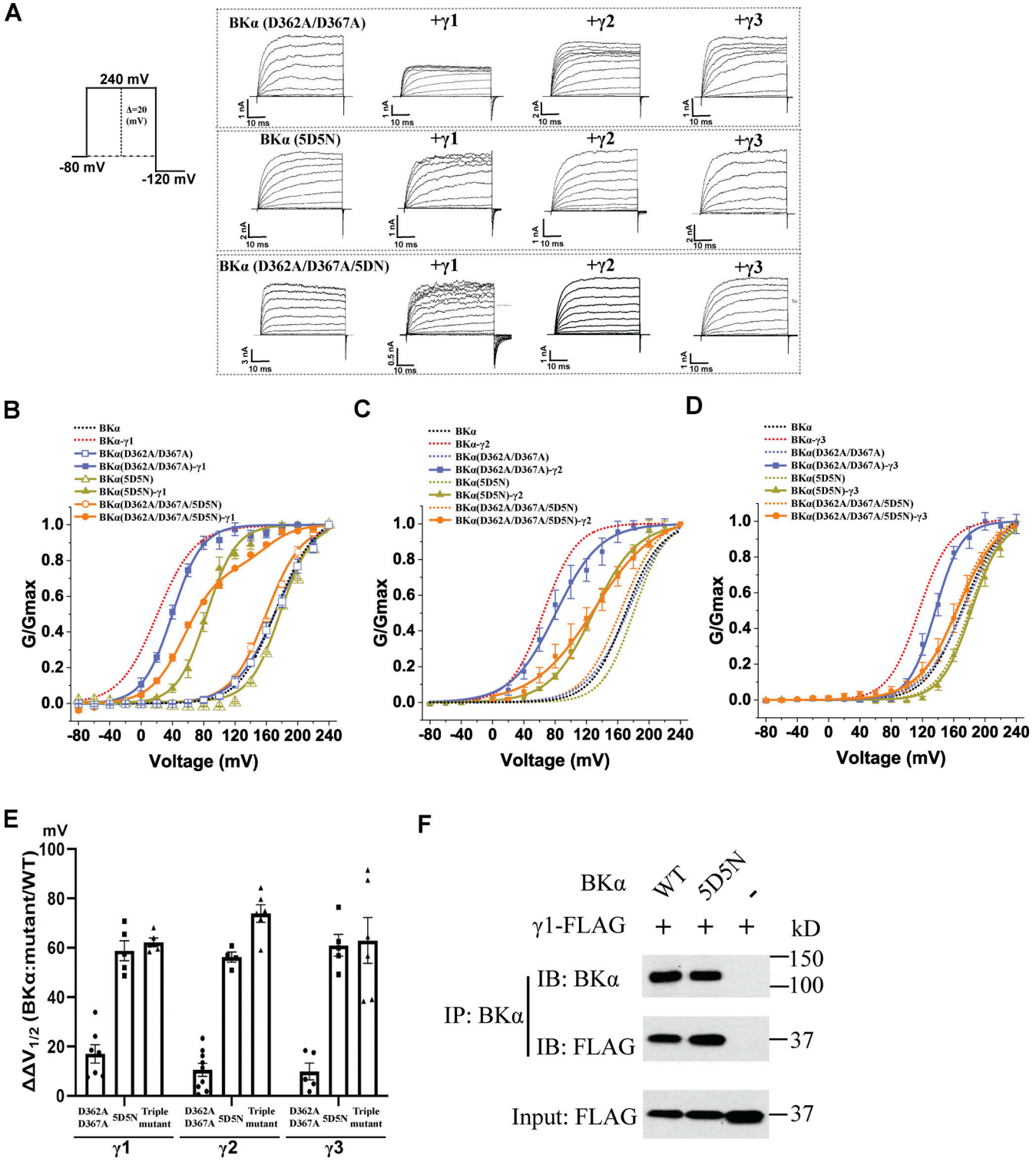


Figure 6. **Effects of $Ca^{2+}$-site mutations on BK channel modulation by γ subunits. (A)** Representative traces of recorded BK channel currents in response to depolarization of the membrane potential from −80 mV in 20-mV steps for selected expression constructs in the virtual absence of $[Ca^{2+}]_i$. **(B–D)** Voltage dependence of BK channel activation for channels formed by BKα mutant (D362A/D367A, 5D5N, or D362A/D367A/5D5N) with and without γ1 (B), γ2 (C), or γ3 (D) subunit in the virtual absence of $[Ca^{2+}]_i$. For comparison, the voltage dependence of WT BK channel activation in the absence and presence of the γ subunit was included in B–D. **(E)** Summary of the BKα mutation-induced reduction ($\Delta\Delta V_{1/2}$) in the $V_{1/2}$-shifting capabilities ($\Delta V_{1/2}$) of the γ1, γ2, and γ3 subunits ($n$ = 4–10). Triple mutant: BKα (D362A/D367A/5D5N). The data obtained with the channel complex of BKα (triple mutant) and γ1 were fitted with a double Boltzmann function. **(F)** Immunoprecipitation of the BKα subunit (WT and 5D5N mutant) with the γ1 subunit. Error bars represent ± SEM. Source data are available for this figure: SourceData F6.

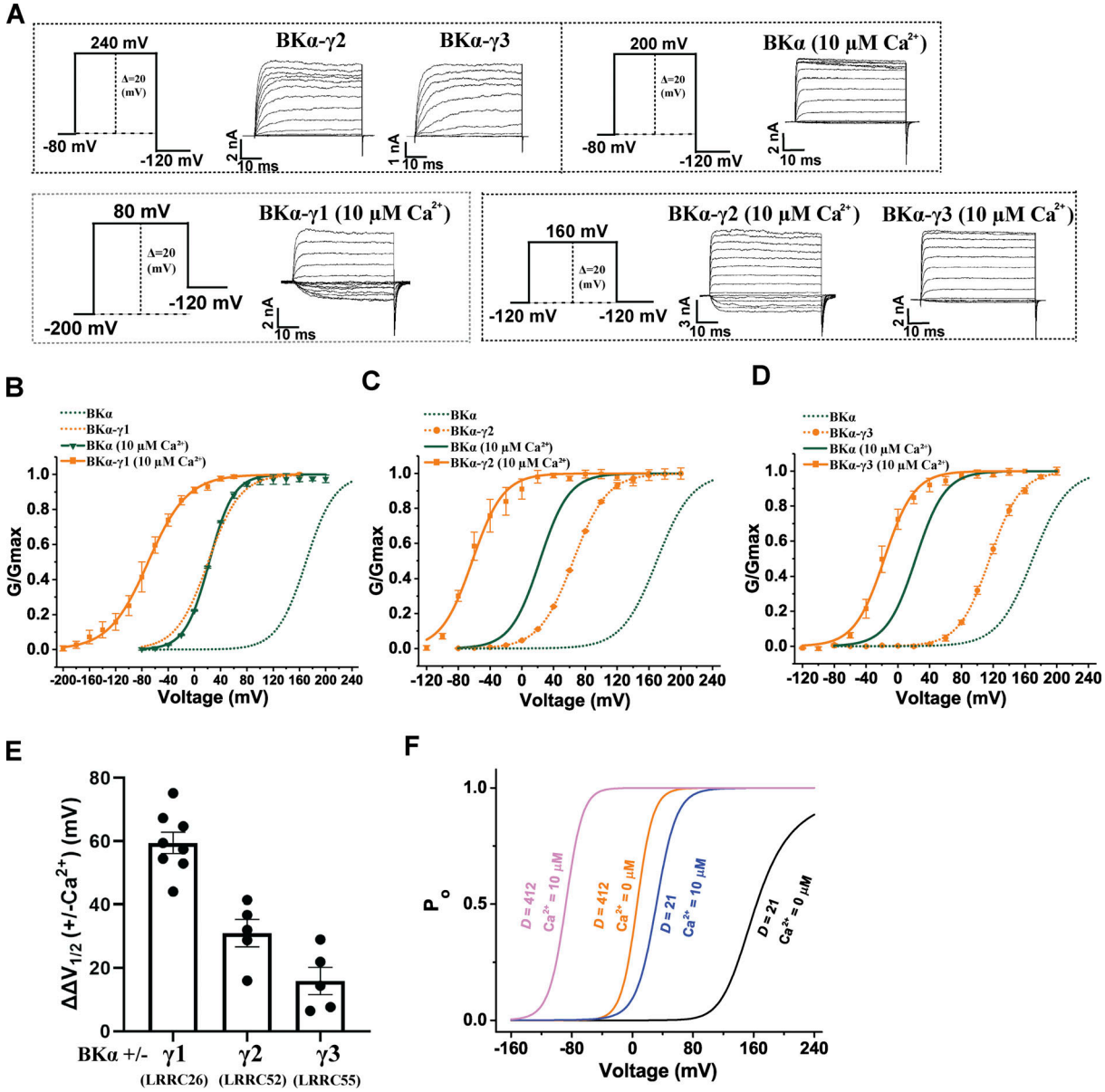


Figure 7. **Effects of $Ca^{2+}$ on BK channel modulation by γ subunits. (A)** Representative current traces of BK channels formed by BKα alone or together with the γ subunit in the virtual absence of $[Ca^{2+}]_i$ (no label) or in the presence of 10 µM $Ca^{2+}$ in response to depolarization of the membrane potential from −80 mV, −120 mV, or −200 mV in 20-mV steps. **(B–D)** Voltage dependence of BK channel activation for channels formed by the BKα and γ1 (E), γ2 (F), or γ3 (G) subunits in the virtual absence of $[Ca^{2+}]_i$ and in the presence of 10 µM $Ca^{2+}$ ($n$ = 4–10). 10 µM $Ca^{2+}$ was included directly in the bath solution. **(E)** Summary of 10 µM $Ca^{2+}$-induced reduction ($\Delta\Delta V_{1/2}$) in the $V_{1/2}$-shifting capabilities ($\Delta V_{1/2}$) of the γ1–3 subunits ($n$ = 4–10). **(F)** Predicted voltage-dependence of BK channel open probability ($P_o$) of unmodulated ($D$ = 21) and modulated ($D$ = 412) BK channel in the absence and presence of 10 µM $Ca^{2+}$ according to the HA allosteric model. The values of the volage-gating parameters were taken from previous reports (Horrigan and Aldrich, 2002; Yan and Aldrich, 2012) as such: $L_0 = 3.6 \times 10^{-6}$, $Z_L$ = 0.29, $J_0$ = 0.048, $Z_J$ = 0.59, $D$ = 21 or 412, $K_D$ = 11, $C$ = 8, $E$ = 2.4. Error bars in B–E represent ± SEM.

Furthermore, the presence of $Ca^{2+}$, charge neutralization of the negatively charged $Ca^{2+}$-bowl, and high ionic strength all induced a significant reduction of or comprehensive loss of the BK channel activation capabilities of the synthetic peptides. This led us to reason that the synthetic peptide mimics of the BKγ subunits' positively charged residue clusters activate BK channels via electrostatic interactions with the highly negatively charged $Ca^{2+}$-bowl site.

It is noteworthy that BK channels can be similarly activated by another positively charged peptide, the HIV-1 Tat. This suggests that BK channels may generally be activated by positively charged peptides unrelated to the γ subunits via interactions with the $Ca^{2+}$-bowl site. This observation has a number of implications. First, cationic cell-penetrating peptides (e.g., HIV-1 Tat) that are broadly used for cellular delivery of molecules may activate BK channels if they accumulate intracellularly at a high enough concentration. Second, BK channels may be modulated by endogenous intracellular peptides or small proteins that are highly positively charged.

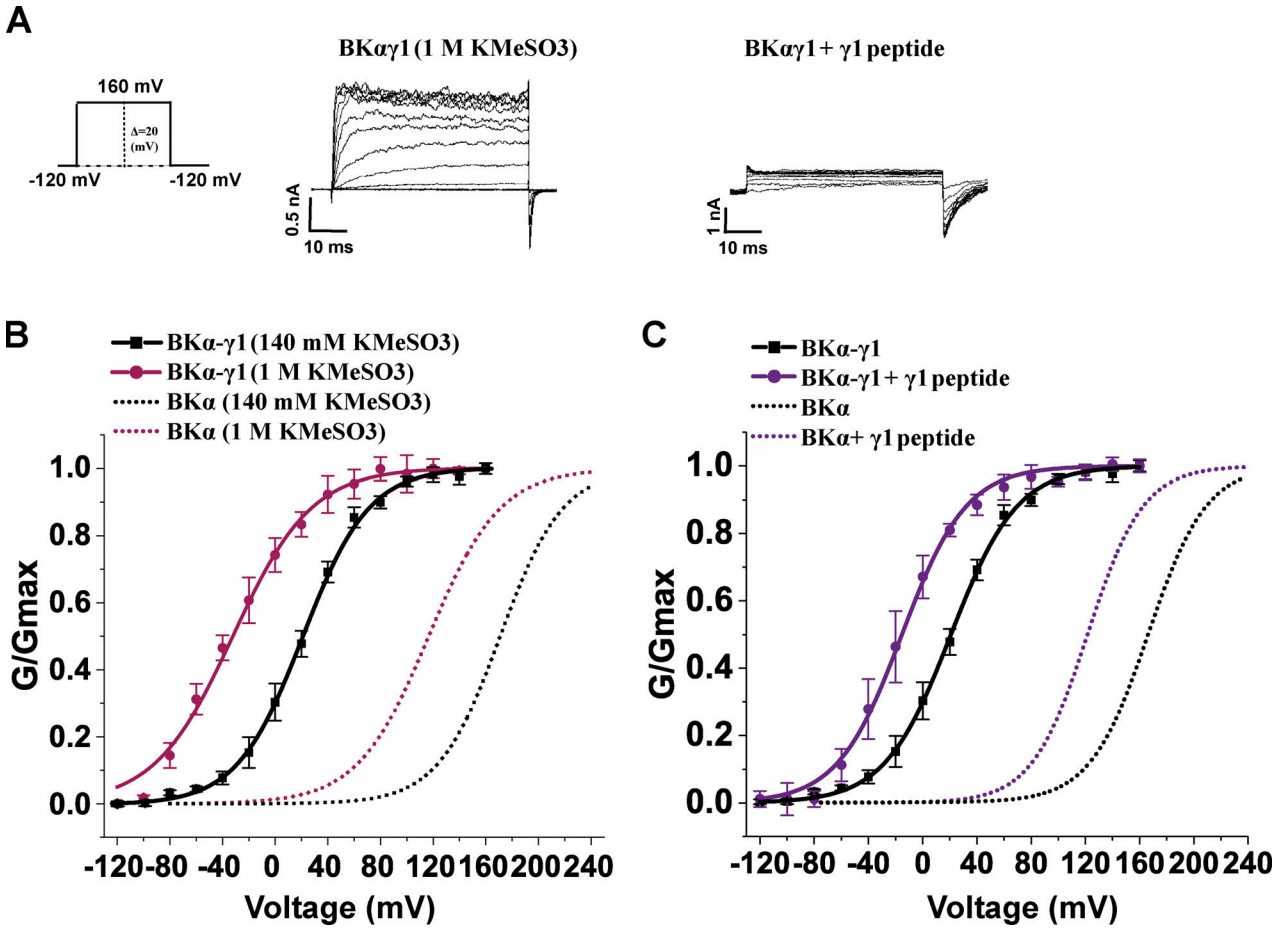


Figure 8. **The effects of ionic strength and the synthetic γ1 peptide mimic on BK channel modulation by the γ1 subunit. (A)** Representative current traces of BK channels formed by the BKα and γ1 subunits under different intracellular conditions (peptide treatment and ionic strength) in response to depolarization of the membrane potential. **(B)** Voltage dependence of the γ1 subunit-complexed BK channel in intracellular solutions of different ionic strengths. **(C)** Voltage dependence of the γ1 subunit-complexed BK channel activation in the absence and presence of the 20 μM γ1 peptide. Currents were recorded in the virtual absence of $[Ca^{2+}]_i$. Error bars represent ± SEM.

The present study provides evidence that peptides with two or more clustered positive charges can potentially act as BK channel activators. The peptide sequence (order of the positively charged residues) likely plays only a minor role because the peptides tested in this study were all different in sequence yet showed similar effects. The γ2 and γ3 peptides have a similar length and number of positive charges but different sequences. Similarly, the γ1 and Tat peptides also have a similar length and number of positive charges but very different sequences. The mechanism of BK channel activation by positively charged peptides could be analogous to those by divalent cations including $Ca^{2+}$, $Sr^{2+}$, and $Ba^{2+}$ as they all involve interactions at the $Ca^{2+}$-bowl site (Zeng et al., 2005; Zhou et al., 2012). Similar to previously reported positively charged small chemicals and peptides (e.g., tetrabutylammonium and enhanced ball peptide; Li and Aldrich, 2006), the positively charged peptides tested in this study also act as effective blockers of BK channels. However, the peptide's channel-activation and channel-blockade effects involve distinct mechanisms. The latter should occur at the channel pore in the membrane as it is voltage-dependent with practically no inhibitory effect on tail currents recorded at very negative voltages. Although a channel blocker can potentially have some channel-activating effect if its presence in the pore impedes channel closure, such a blockade-induced activating effect must be insignificant or minor compared with the overall channel-activating effect observed for the peptides tested in this study.

The C-terminal positively charged regions of intact γ subunits and the corresponding synthetic peptide mimics demonstrated similarities in their activating effects on BK channels. The γ1 and γ3 subunits' C-terminal positively charged tails and their corresponding synthetic positively charged peptide mimics all exhibit ~40 mV $V_{1/2}$-shifting capabilities during BK channel modulation. The $V_{1/2}$-shifting capabilities of the γ subunits and synthetic peptides were similarly compromised in the presence of $Ca^{2+}$ and charge neutralization of the $Ca^{2+}$-bowl site. However, the C-terminal positively charged regions of intact γ subunits and the corresponding synthetic peptide mimics must differ in their BK channel activating mechanisms. Unlike its synthetic peptide mimic, the intact γ1 subunit's BK channel modulatory function was insensitive to high ionic strength. Moreover, a noncompetitive relationship was observed between

the intact γ1 subunit and its synthetic peptide mimic on activation of BK channels. The $Ca^{2+}$-induced reduction in $V_{1/2}$ shifting capability of the γ1 subunit could be caused by the allosteric nature of BK channel gating according to the HA model (Horrigan and Aldrich, 2002) assuming that the γ1 subunit mainly affects the allosteric coupling between the voltage sensors and pore gates as previously proposed (Yan and Aldrich, 2010).

Interestingly, charge neutralization at the $Ca^{2+}$-bowl site reduced BK channel modulation by γ subunits. Given that the 5D5N mutation itself had little effect on BK channel gating in the absence of $Ca^{2+}$, the nonadditive effects of the mutation and the γ subunits on BK channels suggest the presence of interactions between the γ subunits and the $Ca^{2+}$-bowl site. In the absence of a 3-D structure of the BKα/γ complex, the spatial relationship between the γ1 subunit's C-terminal positively charged region and the $Ca^{2+}$-bowl site is unknown. Given the heavily charged characteristics of these two regions, long-distance electrostatic interactions remain plausible, even if they are spatially separated. However, modulation of the BK channel's voltage gating by the γ1 subunit was not significantly affected by changes in ionic strength, indicating the likely lack of an electrostatic mechanism in γ1 subunit-modulation of BK channel gating. Given the indispensable role of the BKα and γ subunits' intracellular regions in BK channel modulation by the γ subunits, the electrostatic interactions between them might be not involved in channel gating but necessary for proper coassembly (e.g., proper orientation of the γ1 subunit's single TM segment within the BKα/γ complex) during the protein complex formation. Although alterations in the intracellular regions of the BKα and γ subunits (e.g., neutralization of the $Ca^{2+}$-bowl site, deletion of BKα subunit's whole intracellular region, or neutralization/deletion of the γ subunit's C-terminal positively charged region) cannot disrupt the apparent association between the BKα and γ1 subunits, they could result in nonoptimal or improper coassembly and thus a reduction or full loss in the modulatory function of the γ1 subunit. In this scenario, the $V_{1/2}$-shifting capability of the γ1 subunit in the mature (i.e., already co-assembled) BKα/γ1 channel complex is insensitive to changes in ionic strength and the presence of positively charged peptides.

In summary, we have found that the intracellular C-terminal region of BKα is indispensable for BK channel modulation by the γ subunit. We have identified that positively charged small peptides corresponding to the tails of γ subunits stimulate BK channels likely via a mechanism of electrostatic interactions with the $Ca^{2+}$-bowl site. Our observation of the channel-activating effect of the cationic cell–penetrating HIV-1 Tat peptide suggests the potential existence of $Ca^{2+}$-bowl site–mediated BK channel activation by exogenous and endogenous positively charged peptides or small proteins. Furthermore, we have revealed a role for the $Ca^{2+}$-bowl site in BK channel modulation by γ subunits, although the precise underlying mechanism remains to be determined.

### Data availability

All relevant data are available in the published article.

## Acknowledgments

Christopher J. Lingle served as editor.

We thank Donald R. Norwood at the Research Medical Library of MD Anderson Cancer Center for editing this article.

This work was supported by National Institutes of Health grants NS078152 (to J. Yan) and GM127332 (to J. Yan) and Science Foundation Ireland 21/FFP-A/9209 (to M.A. Hollywood).

Author contribution: G. Chen, Q. Li, and J. Yan designed experiments and analyzed data. G. Chen and Q. Li performed experiments. T.I. Webb and M.A. Hollywood provided a key reagent and edited the manuscript. G.C. and J.Y. wrote the manuscript.

Disclosures: The authors declare no competing interests exist.

Submitted: 30 July 2022
Revised: 12 January 2023
Revised: 4 April 2023
Revised: 6 April 2023
Accepted: 13 April 2023

## References

Aoki, Y., and G. Tosato. 2004. HIV-1 Tat enhances Kaposi sarcoma-associated herpesvirus (KSHV) infectivity. *Blood*. 104:810–814. https://doi.org/10.1182/blood-2003-07-2533

Bailey, C.S., H.J. Moldenhauer, S.M. Park, S. Keros, and A.L. Meredith. 2019. *KCNMA1*-linked channelopathy. *J. Gen. Physiol.* 151:1173–1189. https://doi.org/10.1085/jgp.201912457

Brenner, R., Q.H. Chen, A. Vilaythong, G.M. Toney, J.L. Noebels, and R.W. Aldrich. 2005. BK channel β4 subunit reduces dentate gyrus excitability and protects against temporal lobe seizures. *Nat. Neurosci.* 8:1752–1759. https://doi.org/10.1038/nn1573

Brenner, R., G.J. Peréz, A.D. Bonev, D.M. Eckman, J.C. Kosek, S.W. Wiler, A.J. Patterson, M.T. Nelson, and R.W. Aldrich. 2000. Vasoregulation by the β1 subunit of the calcium-activated potassium channel. *Nature*. 407:870–876. https://doi.org/10.1038/35038011

Budelli, G., Y. Geng, A. Butler, K.L. Magleby, and L. Salkoff. 2013. Properties of Slo1 $K^+$ channels with and without the gating ring. *Proc. Natl. Acad. Sci. USA*. 110:16657–16662. https://doi.org/10.1073/pnas.1313433110

Chen, G., Q. Li, and J. Yan. 2022. The leucine-rich repeat domains of BK channel auxiliary γ subunits regulate their expression, trafficking, and channel-modulation functions. *J. Biol. Chem.* 298:101664. https://doi.org/10.1016/j.jbc.2022.101664

Du, W., J.F. Bautista, H. Yang, A. Diez-Sampedro, S.A. You, L. Wang, P. Kotagal, H.O. Lüders, J. Shi, J. Cui, et al. 2005. Calcium-sensitive potassium channelopathy in human epilepsy and paroxysmal movement disorder. *Nat. Genet.* 37:733–738. https://doi.org/10.1038/ng1585

Du, X., J.L. Carvalho-de-Souza, C. Wei, W. Carrasquel-Ursulaez, Y. Lorenzo, N. Gonzalez, T. Kubota, J. Staisch, T. Hain, N. Petrossian, et al. 2020. Loss-of-function BK channel mutation causes impaired mitochondria and progressive cerebellar ataxia. *Proc. Natl. Acad. Sci. USA*. 117:6023–6034. https://doi.org/10.1073/pnas.1920008117

Dudem, S., R.J. Large, S. Kulkarni, H. McClafferty, I.G. Tikhonova, G.P. Sergeant, K.D. Thornbury, M.J. Shipston, B.A. Perrino, and M.A. Hollywood. 2020. LINGO1 is a regulatory subunit of large conductance, $Ca^{2+}$-activated potassium channels. *Proc. Natl. Acad. Sci. USA*. 117:2194–2200. https://doi.org/10.1073/pnas.1916715117

Gonzalez-Perez, V., and C.J. Lingle. 2019. Regulation of BK channels by beta and gamma subunits. *Annu. Rev. Physiol.* 81:113–137. https://doi.org/10.1146/annurev-physiol-022516-034038

Gonzalez-Perez, V., P.L. Martinez-Espinosa, M. Sala-Rabanal, N. Bharadwaj, X.M. Xia, A.C. Chen, D. Alvarado, J.K. Gustafsson, H. Hu, M.A. Ciorba, and C.J. Lingle. 2021. Goblet cell LRRC26 regulates BK channel activation and protects against colitis in mice. *Proc. Natl. Acad. Sci. USA*. 118:e2019149118. https://doi.org/10.1073/pnas.2019149118

Gonzalez-Perez, V., X.M. Xia, and C.J. Lingle. 2014. Functional regulation of BK potassium channels by γ1 auxiliary subunits. *Proc. Natl. Acad. Sci. USA*. 111:4868–4873. https://doi.org/10.1073/pnas.1322123111

Guan, X., Q. Li, and J. Yan. 2017. Relationship between auxiliary gamma subunits and mallotoxin on BK channel modulation. *Sci. Rep.* 7:42240. https://doi.org/10.1038/srep42240

Horrigan, F.T., and R.W. Aldrich. 2002. Coupling between voltage sensor activation, $Ca^{2+}$ binding and channel opening in large conductance (BK) potassium channels. *J. Gen. Physiol.* 120:267–305. https://doi.org/10.1085/jgp.20028605

Li, Q., F. Fan, H.R. Kwak, and J. Yan. 2015. Molecular basis for differential modulation of BK channel voltage-dependent gating by auxiliary γ subunits. *J. Gen. Physiol.* 145:543–554. https://doi.org/10.1085/jgp.201511356

Li, Q., X. Guan, K. Yen, J. Zhang, and J. Yan. 2016. The single transmembrane segment determines the modulatory function of the BK channel auxiliary γ subunit. *J. Gen. Physiol.* 147:337–351. https://doi.org/10.1085/jgp.201511551

Li, Q., and J. Yan. 2016. Modulation of BK channel function by auxiliary beta and gamma subunits. *Int. Rev. Neurobiol.* 128:51–90. https://doi.org/10.1016/bs.irn.2016.03.015

Li, W., and R.W. Aldrich. 2006. State-dependent block of BK channels by synthesized shaker ball peptides. *J. Gen. Physiol.* 128:423–441. https://doi.org/10.1085/jgp.200609521

Liang, L., X. Li, S. Moutton, S.A. Schrier Vergano, B. Cogné, A. Saint-Martin, A.C.E. Hurst, Y. Hu, O. Bodamer, J. Thevenon, et al. 2019. De novo loss-of-function KCNMA1 variants are associated with a new multiple malformation syndrome and a broad spectrum of developmental and neurological phenotypes. *Hum. Mol. Genet.* 28:2937–2951. https://doi.org/10.1093/hmg/ddz117

Meredith, A.L., S.W. Wiler, B.H. Miller, J.S. Takahashi, A.A. Fodor, N.F. Ruby, and R.W. Aldrich. 2006. BK calcium-activated potassium channels regulate circadian behavioral rhythms and pacemaker output. *Nat. Neurosci.* 9:1041–1049. https://doi.org/10.1038/nn1740

Niesner, U., C. Halin, L. Lozzi, M. Günthert, P. Neri, H. Wunderli-Allenspach, L. Zardi, and D. Neri. 2002. Quantitation of the tumor-targeting properties of antibody fragments conjugated to cell-permeating HIV-1 TAT peptides. *Bioconjug. Chem.* 13:729–736. https://doi.org/10.1021/bc025517+

Park, S.M., C.E. Roache, P.H. Iffland II, H.J. Moldenhauer, K.K. Matychak, A.E. Plante, A.G. Lieberman, P.B. Crino, and A. Meredith. 2022. BK channel properties correlate with neurobehavioral severity in three *KCNMA1*-linked channelopathy mouse models. *Elife*. 11:e77953. https://doi.org/10.7554/eLife.77953

Rizzuti, M., M. Nizzardo, C. Zanetta, A. Ramirez, and S. Corti. 2015. Therapeutic applications of the cell-penetrating HIV-1 Tat peptide. *Drug Discov. Today*. 20:76–85. https://doi.org/10.1016/j.drudis.2014.09.017

Sausbier, M., H. Hu, C. Arntz, S. Feil, S. Kamm, H. Adelsberger, U. Sausbier, C.A. Sailer, R. Feil, F. Hofmann, et al. 2004. Cerebellar ataxia and Purkinje cell dysfunction caused by $Ca^{2+}$-activated $K^+$ channel deficiency. *Proc. Natl. Acad. Sci. USA*. 101:9474–9478. https://doi.org/10.1073/pnas.0401702101

Schreiber, M., and L. Salkoff. 1997. A novel calcium-sensing domain in the BK channel. *Biophys. J.* 73:1355–1363. https://doi.org/10.1016/S0006-3495(97)78168-2

Shao, L.R., R. Halvorsrud, L. Borg-Graham, and J.F. Storm. 1999. The role of BK-type $Ca^{2+}$-dependent $K^+$ channels in spike broadening during repetitive firing in rat hippocampal pyramidal cells. *J. Physiol.* 521:135–146. https://doi.org/10.1111/j.1469-7793.1999.00135.x

Tao, X., and R. MacKinnon. 2019. Molecular structures of the human Slo1 $K^+$ channel in complex with β4. *Elife*. 8:e51409. https://doi.org/10.7554/eLife.51409

Typlt, M., M. Mirkowski, E. Azzopardi, L. Ruettiger, P. Ruth, and S. Schmid. 2013. Mice with deficient BK channel function show impaired prepulse inhibition and spatial learning, but normal working and spatial reference memory. *PLoS One*. 8:e81270. https://doi.org/10.1371/journal.pone.0081270

Webb, T.I., A.S. Kshatri, R.J. Large, A.M. Akande, S. Roy, G.P. Sergeant, N.G. McHale, K.D. Thornbury, and M.A. Hollywood. 2015. Molecular mechanisms underlying the effect of the novel BK channel opener GoSlo: Involvement of the S4/S5 linker and the S6 segment. *Proc. Natl. Acad. Sci. USA*. 112:2064–2069. https://doi.org/10.1073/pnas.1400555112

Wu, Y., Y. Yang, S. Ye, and Y. Jiang. 2010. Structure of the gating ring from the human large-conductance $Ca^{2+}$-gated $K^+$ channel. *Nature*. 466:393–397. https://doi.org/10.1038/nature09252

Xia, X.M., X. Zeng, and C.J. Lingle. 2002. Multiple regulatory sites in large-conductance calcium-activated potassium channels. *Nature*. 418:880–884. https://doi.org/10.1038/nature00956

Yan, J., and R.W. Aldrich. 2010. LRRC26 auxiliary protein allows BK channel activation at resting voltage without calcium. *Nature*. 466:513–516. https://doi.org/10.1038/nature09162

Yan, J., and R.W. Aldrich. 2012. BK potassium channel modulation by leucine-rich repeat-containing proteins. *Proc. Natl. Acad. Sci. USA*. 109:7917–7922. https://doi.org/10.1073/pnas.1205435109

Yang, C., V. Gonzalez-Perez, T. Mukaibo, J.E. Melvin, X.M. Xia, and C.J. Lingle. 2017. Knockout of the LRRC26 subunit reveals a primary role of LRRC26-containing BK channels in secretory epithelial cells. *Proc. Natl. Acad. Sci. USA*. 114:E3739–E3747. https://doi.org/10.1073/pnas.1703081114

Zeng, X.H., X.M. Xia, and C.J. Lingle. 2005. Divalent cation sensitivity of BK channel activation supports the existence of three distinct binding sites. *J. Gen. Physiol.* 125:273–286. https://doi.org/10.1085/jgp.200409239

Zhang, G., S.Y. Huang, J. Yang, J. Shi, X. Yang, A. Moller, X. Zou, and J. Cui. 2010. Ion sensing in the RCK1 domain of BK channels. *Proc. Natl. Acad. Sci. USA*. 107:18700–18705. https://doi.org/10.1073/pnas.1010124107

Zhou, Y., X.H. Zeng, and C.J. Lingle. 2012. Barium ions selectively activate BK channels via the $Ca^{2+}$-bowl site. *Proc. Natl. Acad. Sci. USA*. 109:11413–11418. https://doi.org/10.1073/pnas.1204444109